Accepted Manuscript

Hydrological natural inflow and climate variables: Time and frequency causality analysis

Xu Huang, Paula Medina Maçaira, Hossein Hassani, Fernando Luiz Cyrino Oliveira, Gurjeet Dhesi

PII: S0378-4371(18)31210-X
DOI: https://doi.org/10.1016/j.physa.2018.09.079
Reference: PHYSA 20140

To appear in: *Physica A*

Received date : 3 June 2018
Revised date : 24 August 2018

Please cite this article as: X. Huang, et al., Hydrological natural inflow and climate variables: Time and frequency causality analysis, *Physica A* (2018), https://doi.org/10.1016/j.physa.2018.09.079

Hydrological Natural Inflow and Climate Variables: Time and Frequency Causality Analysis

Xu Huang[1], Paula Medina Maçaira[2], Hossein Hassani[3*], Fernando Luiz Cyrino Oliveira[2] and Gurjeet Dhesi[4]

*corresponding author: hassani.stat@gmail.com

[1] Faculty of Business and Law, De Montfort University, Leicester, UK.

[2] Department of Industrial Engineering, Pontifical Catholic University of Rio de Janeiro, Brazil.

[3] Research Institute of Energy Management and Planning, University of Tehran, Tehran, Iran.

[4] School of Business, London South Bank University, London, UK.

Abstract

Numbers of studies have proved the significant influence of climate variables on hydrological series. Considering the pivotal role of the hydroelectric power plants play in the electricity production in Brazil this paper considers the natural hydrological inflow data from 15 major basins and 8 climate variables containing 7 El Niño Southern Oscillation proxies and the sunspot numbers. The causal relationships between hydrological natural inflows and climate variables are investigated by adopting and comparing 5 different causality detection methods (Granger Causality test, Frequency Domain Causality test, Convergent Cross Mapping Causality test, Single Spectrum Analysis (SSA) Causality test and Periodic Autoregressive Model Causality test) that cover both well established and novel empirical approaches. Both time domain and frequency domain causality tests gain valid evidences of unidirectional causality for a group of series; CCM achieved unidirectional causality for 18% of pairs and overwhelmingly indicated the opposite direction of causality; a mixture of results are concluded by SSA causality test; PAR based causality test obtained six unidirectional causality, but only one is really significant.

Keywords: Hydrological Natural Inflow; Climate Variables; Causality Detection; Granger Causality; Frequency Domain Causality; Convergent Cross Mapping; Single Spectrum Analysis; Periodic Autoregressive Model.

Nomenclature

CCM	Convergent Cross Mapping.
EDM	Empirical Dynamic Modeling.
$ENSO$	El Niño-Southern Oscillation.
GC	Granger Causality Test.
$NGDC$	National Geophysical Data Center.
$NOAA$	National Oceanic and Atmospheric Administration.
ONI	Oceanic Niño Index.
PAR	Periodic Autoregressive Model.
$PARX$	Periodic Autoregressive Model with One Exogenous Variable.
$RMSE$	Root Mean Square Error.
SOI	Southern Oscillation Index.
SSA	Singular Spectrum Analysis.
SST	Sea Surface Temperature.

1 Introduction

In Brazil there are 1268 hydroelectric power plants in operation, corresponding to 65% of total installed capacity and responsible for 73% of electricity production in 2016 [1]. This kind of power plant produces electricity by harnessing a river's hydraulic potential so the electricity generation depends directly on hydrological regimes.

Since the 90s there are several studies showing that not only there is an influence of climate variables like El Niño-Southern Oscillation (ENSO) on hydrological series [2–6, 8], but also that when correlation is taken into account there is improvement in the forecasting/modelling exercise of inflow time series [9–13], for instance, storm tides data at the Baltic Sea in [14] and stream flow data of the East River basin of China in [15] by adopting the significant Hurst exponent [16], which has also been applied in birth time series [17]. Another recent research considered Hurst exponent in analyzing hydro-geological series can be found in [18].

This paper aims to establish comprehensive causality analyses between natural inflow and climate variables in Brazil by embracing and comparing both well established and advanced causality detection methods, including time domain Granger causality (GC) test [19], frequency domain causality test [20], Convergent Cross Mapping (CCM) [21], Singular Spectrum Analysis (SSA) based causality test [22–25] and the Periodic Autoregressive model (PAR) based causality test [26, 27].

Most of the works previously cited study the influence of ENSO events using the Sea Surface Temperature (SST) variable for the Northeast region of Brazil, ignoring others geographic regions and also other variables that possibly indicate a proxy for ENSO. In this paper, all the fifteen Brazil major basins are considered to test the causality with more than seven ENSO proxies and the Sunspot climate event.

The remainder of this paper is organized such that the background of this study is presented in Section 2; the causality detection techniques adopted in this paper are briefly summarized in

Section 3; Section 4 introduces the data and summarizes the descriptive statistics along with correlation analyses; the detailed causality test results by different methods are listed in Section 5; the paper concludes in Section 6 with proposals of future research.

2 Background

It is possible to find several studies that identify the influence of ENSO events in the Brazilian river basins, but none of them apply any type of causality test. Amarasekera et al. [2] concludes that the annual discharges of the Amazon river is weakly and negatively correlated with the equatorial Pacific Sea Surface Temperature (SST) anomaly, while the the Paraná river shows a strong and positive correlation. Dettinger & Diaz [3] uses El Niño variations to characterize geographic differences in the seasonality and year-to-year variability of stream flow from several sites around the world, and shows that the Amazon basin is drier-than-normal in El Niño years accordingly to Southern Oscillation Index (SOI) and North Atlantic Oscillation (NAO) [28] index. Foley et al. [4] shows that during the El Niño there is a decrease in the Amazon and Tocantins river discharge, and the opposite during the La Niña. Berri et al. [5] presents that exactly the opposite happens in Paraná river, and during El Niño the average inflow are always larger than those observed during La Niña events. Garcia & Mechoso [6] concludes that the Amazon, Tocantins, San Francisco, Paraguay, Paraná river stream flows shows El Niño-like periodicities. Soares et al. [8] notice that the sub-basins of the southern Brazilian regions showed positive variations in water production during El Niño, while the Amazon basin showed no response.

Souza Filho [9] shows that the correlation between climate and hydrological variables is beneficial for the prediction of reservoir inflows in Ceará. Cardoso & Silva Dias [10] use the SST index to show that there is improvement in the reservoir inflow forecasting of Paraná River. Lima & Damien [11] apply dynamic linear models to predict the inflow of the Brazil fifteen main basins using precipitation and an El Niño index. Maçaira et al. [12] developed a causal PAR model to estimate the influence between several El Niño indices and the inflow time series of some Brazilian locations. Silveira et al. [13] propose the Periodic Autoregressive model with one exogenous variable (PARX) to simultaneously predict all natural inflows of the National Interconnected System.

Apart from the significance of studying the causal links between natural inflow and climate factors, this paper has adopted 5 different causality detection techniques covering both well established and advanced time series analysis methods (note that the detailed introduction of these methods are summarized in section 3). It worth to be noted as another contribution of this paper that it comprehensively investigates the causal relationship with the most up to date time series analysis techniques to our knowledge.

The well established and widely applied GC approach enables researchers to evaluate dependence relationship, mostly linear, among factors in a complex system. It brings insights on whether the changes of one factor have relationship with the changes of another factor in the

current sequence or after specific lag of time. However, it assumes linearity and separability for the selected variables in the model and the nonlinear applicability is limited. The frequency domain causality test extends the GC approach to identify the causality for each frequency instead of a single statistics for the whole time series, whilst the restricted assumptions and nonlinear applicability maintain. In addition, by adopting the advanced time series analysis techniques like SSA and CCM, this paper also explores the causality detection from the aspect of nonlinearity and other complex dynamics. These advanced non-parametric techniques are relatively new and have no assumptions of linear or restricted nonlinear model. They are designed to be widely applicable and assumption free with straightforward way of thinking and implementing. By adopting these advanced methods, this paper seeks to further distinguish possible causal relationships that the empirical tests cannot achieve or fall short at. In general, to the best of our knowledge, this paper is the first attempt that applies and compares all these five causality detection methods to date. Moreover, for most of the advanced methods, it is also the initial implementation study on the natural inflow and climate variables in Brazil.

3 Causality Detection Methods

3.1 Time Domain Granger Causality Test

GC test [19] is the most generally accepted and significant method for causality analyses in various disciplines. The regression formulation of Granger causality states that vector X_i is the cause of vector Y_i if the past values of X_i are helpful in predicting the future value of Y_i, two regressions are considered as follows:

$$Y = \sum_{t=1}^{T} \alpha_t Y_{i-t} + \varepsilon_{1i}, \tag{1}$$

$$Y = \sum_{t=1}^{T} \alpha_t Y_{i-t} + \sum_{t=1}^{T} \beta_t X_{i-t} + \varepsilon_{2i}, \tag{2}$$

where $i = 1, 2, \cdots, N$ (N is the number of observations), T is the maximal time lag, α and β are vectors of coefficients, ε is the error term. The first regression is the model that predicts Y_i by using the history of Y_i only, while the second regression involves both X_i and Y_i. Therefore, the conclusion of existing causality is conducted if the second model is a significantly better model than the first one.

3.2 Frequency Domain Causality Test

The frequency domain causality test is the extension of time domain GC test that identifies the causality between different variables for each frequency. In order to briefly introduce the testing methodology, we mainly follow [20, 29].

It is assumed that two dimensional vector containing X_i and Y_i (where $i = 1, 2, \cdots, N$ and N is the number of observations) with a finite-order Vector Auto-regression Model representative

of order p,

$$\Theta(R)\begin{pmatrix} Y_i \\ X_i \end{pmatrix} = \begin{pmatrix} \Theta_{11}(R) & \Theta_{12}(R) \\ \Theta_{21}(R) & \Theta_{22}(R) \end{pmatrix}\begin{pmatrix} Y_i \\ X_i \end{pmatrix} + \mathcal{E}_i, \tag{3}$$

where $\Theta(R) = I - \Theta_1 R - ... - \Theta_p R_p$ is a 2×2 lag polynomial and $\Theta_1, ..., \Theta_p$ are 2×2 autoregressive parameter matrices, with $R^k X_i = X_{i-k}$ and $R^k Y_i = Y_{i-k}$. The error vector $\mathcal{E}$ is white noise with zero mean, and $E(\mathcal{E}_i \mathcal{E}_i') = \mathbf{Z}$, where $\mathbf{Z}$ is positive definite matrix. The moving average representative of the system is

$$\begin{pmatrix} Y_i \\ X_i \end{pmatrix} = \Psi(R)\eta_i = \begin{pmatrix} \Psi_{11}(R) & \Psi_{12}(R) \\ \Psi_{21}(R) & \Psi_{22}(R) \end{pmatrix}\begin{pmatrix} \eta_{1i} \\ \eta_{2i} \end{pmatrix}, \tag{4}$$

with $\Psi(R) = \Theta(R)^{-1}\mathbf{G}^{-1}$ and $\mathbf{G}$ is the lower triangular matrix of the Cholesky decomposition $\mathbf{G}'\mathbf{G} = \mathbf{Z}^{-1}$, such that $E(\eta_t \eta_t') = I$ and $\eta_i = \mathbf{G}\mathcal{E}_i$. The causality test developed in [29] can be written as:

$$C_{X\Rightarrow Y}(\gamma) = log\left[1 + \frac{|\Psi_{12}(e^{-i\gamma})|^2}{|\Psi_{11}(e^{-i\gamma})|^2}\right]. \tag{5}$$

However, according to this framework, no Granger causality from X_i to Y_i at frequency γ corresponds to the condition $|\Psi_{12}(e^{-i\gamma})| = 0$, this condition leads to

$$|\Theta_{12}(e^{-i\gamma})| = |\Sigma_{k=1}^{p}\Theta_{k,12}\cos(k\gamma) - i\Sigma_{k=1}^{p}\Theta_{k,12}\sin(k\gamma)| = 0, \tag{6}$$

where $\Theta_{k,1,2}$ is the $(1,2)th$ element of Θ_k, such that a sufficient set of conditions for no causality is given by [20]

$$\begin{aligned} \Sigma_{k=1}^{p}\Theta_{k,1,2}\cos(k\gamma) &= 0 \\ \Sigma_{k=1}^{p}\Theta_{k,1,2}\sin(k\gamma) &= 0 \end{aligned}, \tag{7}$$

Hence, the null hypothesis of no Granger causality at frequency γ can be tested by using a standard F-test for the linear restrictions (7), which follows an $F(2, B-2p)$ distribution, for every γ between 0 and π, with B begin the number of observations in the series.

3.3 Convergent Cross Mapping

CCM is firstly introduced in [21] that aimed at detecting the causation among time series and provide a better understanding of the dynamical systems that have not been covered by other well established methods like GC. CCM has proven to be an advanced non-parametric technique for distinguishing causation in a dynamical system that contains complex interactions in ecosystem and climate studies [21,30], more details can be found in [31,32]. Some significant rationales of embracing this advanced technique include: CCM is non-parametric approach with no restrictions of assumptions for parametric methods; CCM can distinguish statistically significant causality by considering only two key variables instead of building a complex model by incorporating many possible influential variables based on regression modelling; CCM has remarkable sensitivity at detecting causal links within complex systems whilst not being limited

to linearity or non-linearity; the calculation itself is efficient and comparatively straightforward. CCM is briefly introduced below by mainly following [21].

Assume there are two variables X_i and Y_i, for which X_i has a causal effect on Y_i. CCM test will test the causation by evaluating whether the historical record of Y_i can be used to get reliable estimates of X_i. Given a library set of n points (not necessarily to be the total number of observations N of two variables) and here set $i = 1, 2, \cdots, n$, the lagged coordinates are adopted to generate an E-dimensional embedding state space [33,34], in which the points are the library vector X_i and prediction vector Y_i

$$X_i : \{x_i, x_{i-1}, x_{i-2}, \cdots, x_{i-(E-1)}\}, \tag{8}$$

$$Y_i : \{y_i, y_{i-1}, y_{i-2}, \cdots, y_{i-(E-1)}\}, \tag{9}$$

The $E+1$ neighbors of Y_i from the library set X_i will be selected which actually form the smallest simplex that contains Y_i as an interior point. Accordingly, the forecast is then conducted by this process, which is the nearest-neighbour forecasting algorithm of simplex projection [34]. The optimal E will be evaluated and selected based on the forward performances of these nearby points in an embedding state space.

Therefore, by adopting the essential concept of Empirical Dynamic Modeling (EDM) and generalized Takens' Theorem [33], two manifolds are conducted based on the lagged coordinates of the two variables under evaluation, which are the attractor manifold M_Y constructed by Y_i and respectively, the manifold M_X by X_i. The causation will then be identified accordingly if the nearby points on M_Y can be employed for reconstructing observed X_i. Note that the correlation coefficient ρ is used for the estimates of cross map skill due to its widely acceptance and understanding, additionally, leave-one-out cross-validation is considered a more conservative method and adopted for all evaluations in CCM.

3.4 Singular Spectrum Analysis based Causality Test

As GC formalized the causality concept and claimed causality if the elimination of one variable from a system is harmful for explaining the other variable. Similarity, as can be seen in Figure 1, the SSA based causality analysis is obtained by comparing the forecast values obtained by the univariate procedure–SSA and multivariate process– multivariate SSA (MSSA). Consequently, if the forecasting errors using MSSA are significantly smaller than those of univariate SSA, it is concluded that there is a causal relationship detected between these series. As a nonparametric technique, the SSA causality test is able to capture possible nonlinearities using a data-driven approach without specifying any known functional nonlinear model to the relationship, which in turn, could be incorrectly specified in the first place. Detailed introduction is presented below which mainly follow [25, 35], where also summarize the details of SSA and MSSA formulation and forecasting algorithms.

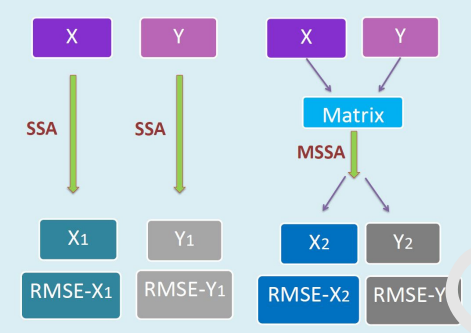

Figure 1: Flowchart of Cause Detection based on SSA Forecasting Accuracy.

Let us consider the procedure for constructing vectors of forecasting error for out-of-sample tests in a two variable case X_N and Y_N by both univariate and multivariate SSA techniques respectively. Firstly, the series $X_N = (x_1, ..., x_N)$ is divided into two separate subseries X_R and X_F that satisfy $X_N = (X_R, X_F)$, where $X_R = (x_1, ..., x_R)$ and $X_F = (x_{R+1}, ..., x_N)$. Same procedure is also conducted for Y_N. The subseries X_R and Y_R are used in the reconstruction step to provide the noise-free series $\tilde{X}_R$ and $\tilde{Y}_R$. The noise-free series are then used for forecasting the subseries X_F and Y_F with the help of the forecasting algorithms (see [25]) of SSA and MSSA respectively. For variable X_N, two different forecasting values of $\hat{X}_F = (\hat{x}_{R+1}, ..., \hat{x}_N)$ by SSA and MSSA are then used for computing the forecasting errors accordingly, which will be the same process in terms of variable Y_N. Therefore, in a multivariate system like this, the vectors of forecasts obtained can be used in computing the forecasting accuracy and therefore conducting the causality analysis between the two variables.

The length of out-of-sample does not have specific limitation, generally considering the simulation scenario, the length of time series for reconstruction will take 2/3 of the whole series and the rest 1/3 is considered as out-of-sample for constructing forecasting error. The separate point to define the out-of-sample size for different series can be chosen respectively, whilst it is important that when it goes to comparing the performances of different techniques based on constructed forecasting error of one specific series, the sizes of reconstruction and out-of-sample for all techniques should be identical. In addition, the choices of window length L and the referring options of numbers of eigenvalues r should also be carefully evaluated in practice of SSA causality tests respectively. Considering this as the first attempt of application, also in order to conduct the most accurate results, all the possibilities of L and its referring choices of r should be applied for both univariate SSA and MSSA processes, then the optimal ones with best performance of forecasting will be chosen to construct the finally cause detection procedure.

Consequently, define the criterion $F_{X|Y} = \Delta X_{F|Y} / \Delta X_F$ corresponding to the forecast of the series X_N in the presence of the series Y_N. Specifically, if $F_{X|Y}$ is small, then having information obtained from the series Y can help to achieve better forecasts of the series X. If $F_{X|Y} < 1$, it is concluded that the information provided by the series Y can be regarded as useful or supportive for forecasting the series X. Alternatively, if the values of $F_{X|Y} \geq 1$, then either there is no

detectable causality between X and Y or the performance of the univariate SSA is better than of the MSSA (this may happen, for example, when the series Y has structural breaks misdirecting the forecasts of X).

3.5 Periodic Autoregressive Model based Causality Test

To perform monthly forecasts and simulation of hydrological series, the classical PAR model has been widely used [26]. This type of model adjusts the series using the estimated parameters of the historical data [36], and does not consider any exogenous information that could affect the hydrological regimes in equation (10). To consider any exogenous variable in the PAR model, there is the Periodic Autoregressive model with one exogenous variable (PARX) as presented in equation (11). PAR models fit for each season an autoregressive term being able to capture the monthly variability of hydrological regimes, this is the main reason for its success for this type of data. The mathematical details of PAR and PARX can be found in [12, 13, 27].

$$\left(\frac{Y_i - \mu_m}{\sigma_m}\right) = \sum_{t=1}^{p_m} \varphi_t^m \left(\frac{Y_{i-t} - \mu_{m-t}}{\sigma_{m-t}}\right) + \varepsilon_t, \tag{10}$$

$$\left(\frac{Y_i - \mu_m}{\sigma_m}\right) = \sum_{t=1}^{p_m} \varphi_t^m \left(\frac{Y_{i-t} - \mu_{m-t}}{\sigma_{m-t}}\right) + \sum_{t=0}^{v_m} \vartheta_t^m X_{i-t} + \varepsilon_t, \tag{11}$$

Where μ_m and σ_m are the average and the standard deviation of season m, respectively; φ_t^m is the t-th autoregressive coefficient of season m, p_m is the order of the autoregressive operator of season m. In (11), X_i is the predictor variable, ϑ_t^m is the autoregressive coefficient and v_m is the order of the autoregressive operator of season m for the predictor variable.

Similar to the SSA based Causality Test, it was developed the PAR based Causality Test that compares the forecasts values obtained by the univariate process PAR and the PARX. If the forecasting errors using PARX are significantly smaller than those of PAR, it is conclude that there is a causality detected among the variables.

4 Data

4.1 The Natural Inflow Series in Brazil

According to the Brazilian Electricity Regulatory Agency (ANEEL) there are fifteen major river basins in Brazil, with an installed capacity of approximately 90 GigaWatts [GW] in 2016, representing 68% of the total installed capacity in the country (Figure 2). The Parana river basin has the highest hydroelectric potential, around 43 GW, which represents 48% of total hydroelectric capacity. It can be further subdivided into six minor basins based on its major rivers - Paranaiba, Grande, Tiete, Parana, Paranapanema and Iguacu.

Figure 2: Major rivers basins in Brazil.(Source: [11])

The historical data available is the natural inflow[1] for each generator, on a monthly basis, starting in January 1931 and ending in December 2015, measured in cubic meters per second $[m^3/\text{s}]$. For generators built after 1931, the National Electric System Operator performs a backward forecasting in order to standardize the records for the hydrothermal dispatch optimization process.

In the major rivers there are around 164 hydroelectric power plants currently in operation [37], and these plants operate in a cascade scheme, see in Figure 3 this cascade scheme for Paranaíba and Grande basins with 19 generators with reservoirs, represented by triangles, and 15 generators with no reservoir (circles). This way decisions taken at the upstream reservoirs will impact the inflow of the downstream reservoirs.

[1]The natural inflow is the average incoming water per unit of time at each generator's reservoir from affluent rivers, lakes and its own drainage area.

Figure 3: Example of a cascade scheme.(Source: Adapted from [1])

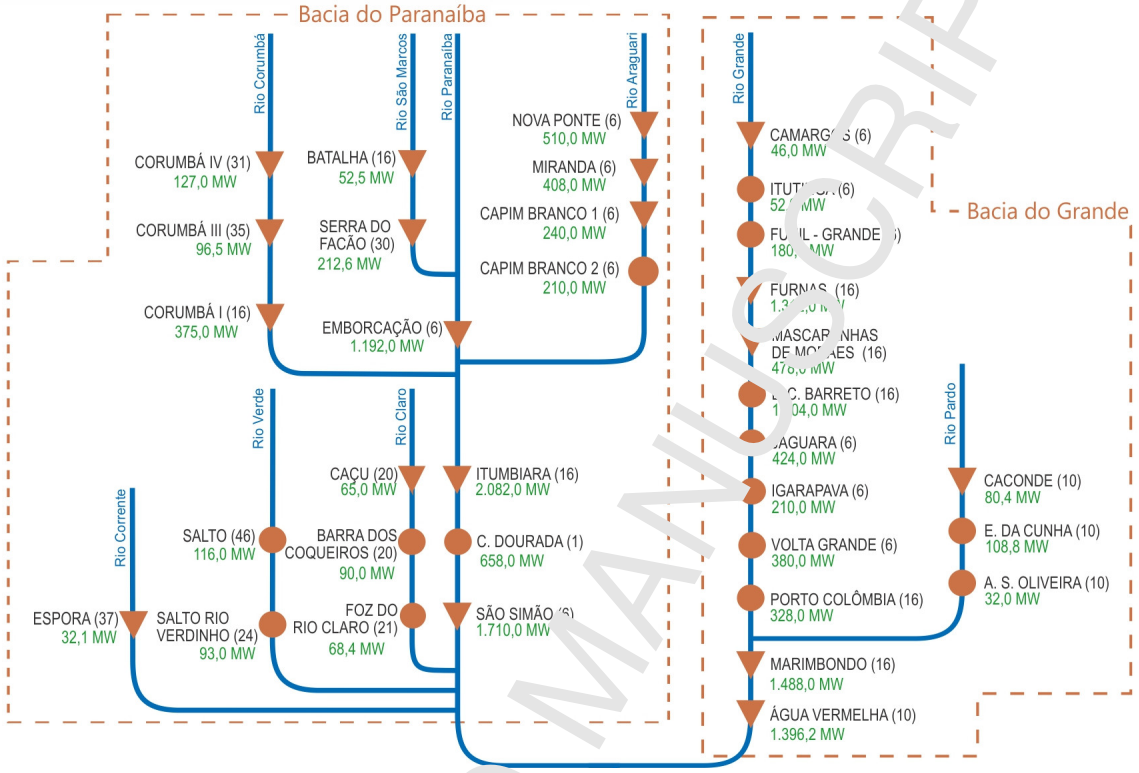

Since there is a cascade scheme, the natural inflow of each generator has to be calculated based on the concept of incremental inflows. For exemplifications reason, assume that Camargos is Generator number 1 and Itutinga is Generator number 2 in Figure 3. If Generator 1 comes first in the cascade, the incremental inflow will be equal to its natural inflow. But, if Generator 2 has 1 upstream, so its incremental inflow will be given by the difference between its natural inflow and the natural inflow of Generator 1. The generators will be grouped by basin creating an equivalent generator with natural inflow equal to the sum of the incremental inflows of all reservoirs belonging to the basin (Figure 4). It is of note that all natural inflow data analyzed in the following sections have been adjusted accordingly considering the cascade scheme.

4.2 Climate Variables

The climate variables were selected trough a literature search. The selected variables are related to El Niño and the Sunspots numbers; the variables representing El Niño/La Niña phenomenon are: Southern Oscillation Index (SOI), Equatorial SOI, Niño variations and Oceanic Niño Index (ONI).

The SOI is calculated based on the difference between the atmospheric pressure at sea level in the regions of Tahiti (in the Western Pacific) and Darwin (Australia, Western Pacific) [38]. The Equatorial SOI measures the average difference of atmospheric pressure at sea level between two regions centered on the equator: Indonesia and East Pacific. The range to indicate the presence

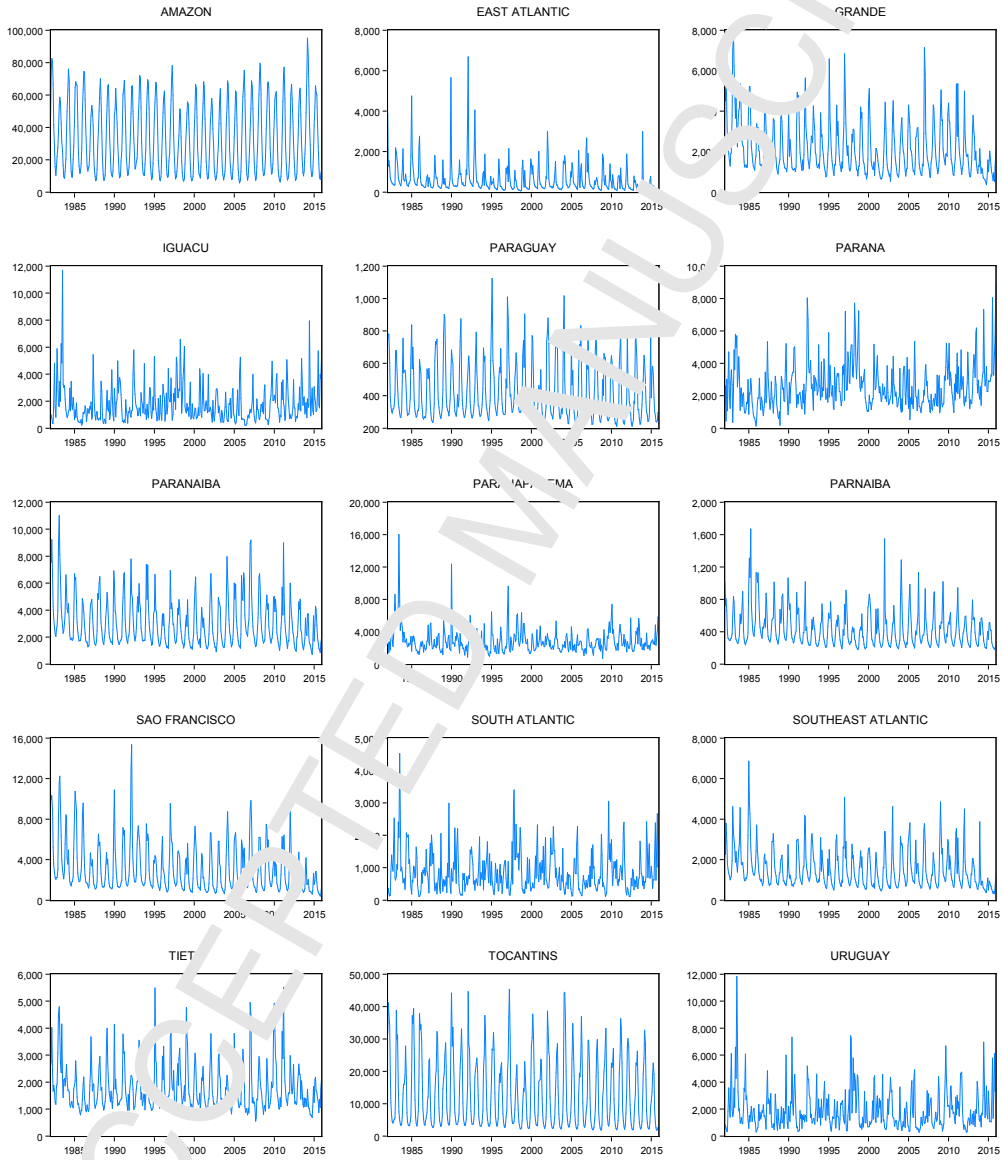

Figure 4: The natural inflow series in Brazil.

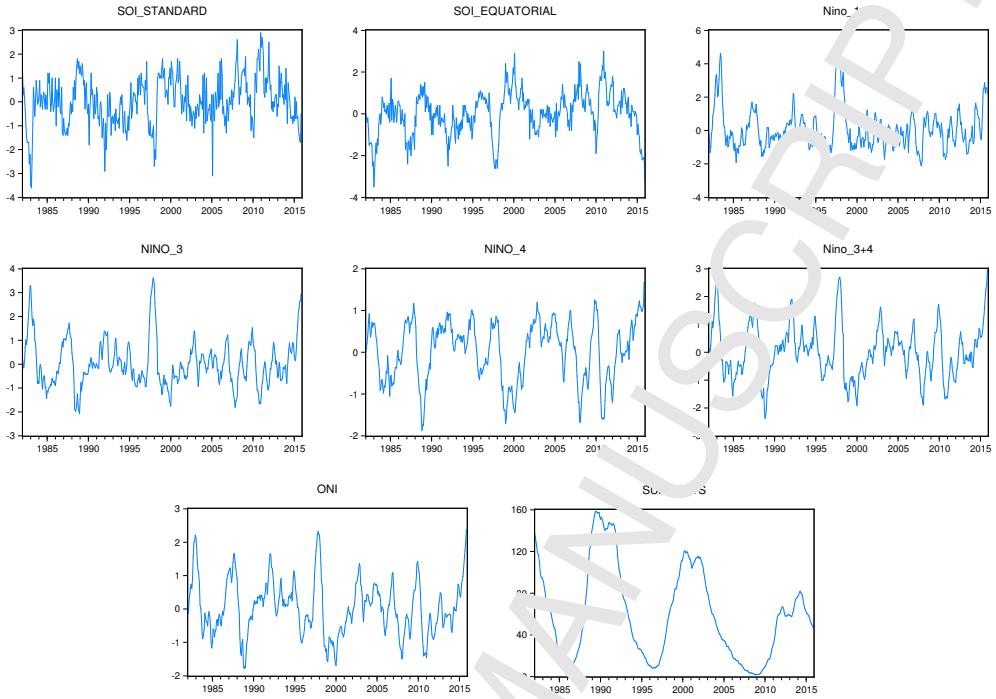

Figure 5: The climate variables in Brazil.

or absence of El Niño/La Niña is the same for both the SOI index and Equatorial SOI. It is also of note that the influence of El Niño in North America indicate a nearly 30 year long cycle due to the different geographical zone [39]. Consecutive periods of negative figures indicate El Niño phenomenon occurrence; meanwhile consecutive positive figures denote the presence of La Niña and values close to zero indicate a normal situation, where none of the two phenomenons occur. The official historical monthly series of these indices are provided by the National Oceanic and Atmospheric Administration (NOAA).

The Sea Surface Temperature (SST) is the water temperature close to the ocean's surface. The SST anomaly, that is, the temperature variation by month, is a proxy for El Niño and La Niña. Thus, this index is used to classify and quantify such phenomena in four Niño regions: Niño 1+2, Niño 3, Niño 4 and Niño 3.4, defined as follows by NOAA in 2014. Through the location of the Niño regions it is possible to conclude that regions Niño 1+2 and Niño 3 better identify temperature anomalies for the Eastern Pacific Ocean sea surface and region Niño 4 for the Western Pacific. The Niño 3.4 region is centralized in the Pacific, which allows a better understanding of anomalies across it. Therefore, currently the Niño 3.4 region is the official measure used to represent SST. However, depending on the study, other regions may be a better alternative. The threshold for the normal state of this index is between $-0.5°C$ and $+0.5°C$. The criteria commonly used to define an El Niño phenomenon consists of five consecutive averages of SST anomalies above $+0.5°C$. Similarly, for La Niña, this criterion remains, but now the

SST anomaly should be below $-0.5°C$. The monthly time series for all regions are provided by NOAA.

The ONI measures the average sea surface temperature anomalies for the region Niño 3.4, removing the existing warming trend on it. According to the NOAA website, multiple centered 30-year based periods are adopted for obtaining ONI values of five successive years. For instance, the 1956-1960 ONI values are based on the 1941-1970 period, while 1936-1965 base period produces the 1950-1955 ONI values. The El Niño and La Niña are indicated in the same manner as the SST index, the time series is monthly and is provided by NOAA.

Sunspots comprehend solar surface regions of high magnetic field, which have considerably lower temperature than its surroundings and thus appear as a dark area. The magnetic flux amount on the sun surface varies over eleven year periods, known as sunspot and solar cycles. During this cycle there is a minimum and a maximum magnetic flux, which is not only difficult to identify the sunspots and but also they appear almost all the time. The cycle reaches its maximum approximately every eleven years, therefore the observed cycle duration corresponds to eleven years.

The number of sunspots calculation is accomplished with the Relative Index American number of sunspots. This index indicates the solar phenomenon occurrence taking into account their relationship with the Earth, including geomagnetic variations and ionosphere effects. The Solar Division from American Association of Variable Star Observers coordinates the data collection program and the analysis of this phenomenon. Thus, the National Geophysical Data Center (NGDC), provides the historical data from the number of sunspots per month since 1749.

Considering the availability of all series and since the SST is only available after 1982, the data used for this paper are at monthly frequency from January 1982 to December 2015. A brief summary table is listed below in Table 1 and the descriptive statistics can be found in Table 2.

Table 1: Summary of tested series.

	Abbreviation	Variable
Natural Inflow Series	AMZ	Amazon
	EAT	East Atlantic
	GRA	Grande
	IGU	Iguacu
	P1	Paranaiba
	P2	Paranapanema
	P3	Parana
	P4	Paraguay
	P5	Parnaiba
	SAT	South Atlantic
	SEAT	Southeast Atlantic
	SF	Sao Francisco
	TIE	Tiete
	TOC	Tocantins
	URU	Uruguay
Climate Variables	SOI_St	Southern Oscillation Index Standard
	SOI_Eq	The Equatorial Southern Oscillation Index
	NN12	Sea Surface Temperature of Niño 1+2 Region
	NN3	Sea Surface Temperature of Niño 3 Region
	NN4	Sea Surface Temperature of Niño 4 Region
	NN34	Sea Surface Temperature of Niño 3.4 Region
	ONI	The Oceanic Niño Index
	SS	Sunspots Number

Table 2: Descriptive statistics of data.

Series	Mean	Median	Maximum	Minimum	Std. Dev.	Skewness	Kurtosis	Obs
AMZ	33553.30	27753.5	95085	5600	21564.07	0.47	1.97	408
EAT	622.75	356	7900	45	746.51	3.67	22.33	408
GRA	2155.66	1721	7938	364	1323.23	1.36	4.79	408
IGU	1802.17	1414	11670	206	1368.56	2.12	10.77	408
P4	425.12	352	1124	212	178.78	1.07	3.42	408
P3	2587.07	2309	8900	130	1368.81	1.35	5.69	408
P1	3094.21	2400	11025	705	1796.74	1.29	4.53	408
P2	2857.46	2504	16004	699	1521.65	3.12	20.81	408
P5	438.33	386.5	1668	178	232.30	1.70	6.71	408
SF	3152.20	2220	15360	406	2481.43	1.55	5.49	408
SAT	868.39	689.5	4524	110	616.66	1.64	7.01	408
SEAT	1535.40	1126	6862	319	975.27	1.56	5.97	408
TIE	1787.3	1549.5	5519	548	849.09	1.64	6.03	408
TOC	13064.57	8229	45317	1772	10943.19	0.93	2.81	408
URU	1900.78	1470	11834	262	1472.04	2.00	9.32	408
SOI_St	0.03	0	2.9	-3.6	1.01	-0.21	3.60	408
SOI_Eq	0.02	0.1	3	-3.5	1.03	-0.37	3.51	408
NN12	0.00	-0.18	4.62	-2.1	1.21	1.32	5.00	408
NN3	0.05	-0.13	3.62	-2.07	0.99	0.95	4.46	408
NN34	0.03	0.005	2.95	-2.38	0.97	0.41	3.25	408
NN4	0.04	0.19	1.67	-1.87	0.72	-0.50	2.49	408
ONI	0.05	-0.01	2.37	-1.78	0.84	0.36	3.00	408
SS	57.12	56.6	158.5	1.7	44.31	0.57	2.24	408

4.3 Correlation Analysis

Prior to the comparison of causality analyses by different methods, the correlation analysis results are here summarized in Table 3 and Table 4. Note that the results are Pearson correlation coefficients respectively considering the empirical status of Pearson approach and ** indicates

significance at the 0.01 level whilst * reflects the 0.05 level.

As can be seen in Table 3, the correlation between natural inflow and climate variables are overwhelmingly weak, except a few weak correlations detected among NN12, NN3, P2, P3, SAT and URU. The correlations between the climate series are also evaluated and summarized in Table 4. Similar conclusions are obtained as expected following the results in [12]: SOI indices hold negative correlation with the others, whilst the El Niño and ONI series indicate strong positive values.

Table 3: Correlation between natural inflow and climate variables.

	AMZ	EAT	GRA	IGU	P1	P2	P3	P4		SAT	SEAT	SF	TIE	TOC	URU
SOI_St	0.06	-0.06	0.00	-0.07	-0.03	-0.09	-0.09	0.09	0.09	-0.13**	0.01	-0.03	0.01	0.06	-0.11*
SOI_Eq	0.03	-0.04	-0.05	-0.22**	-0.05	-0.24**	-0.23**	0.06	[illegible]29	-0.27**	0.01	-0.04	-0.06	0.05	-0.26**
NN12	-0.03	-0.05	0.08	0.37**	0.04	0.36**	0.38**	-0.03	-0.1[illegible]**	0.33**	-0.03	0.02	0.14**	-0.07	0.37**
NN3	-0.06	-0.03	0.03	0.28**	0.04	0.26**	0.31**	-0.[illegible]8	-0.1[illegible]**	0.32**	-0.05	-0.01	0.09	-0.09	0.33**
NN4	-0.03	0.02	-0.06	0.11*	0.01	0.07	0.19**	-0.05	-0.[illegible]8	0.16**	-0.07	-0.02	-0.02	-0.03	0.16**
NN34	-0.06	0.01	0.01	0.20**	0.03	0.18**	0.25**	-0.[illegible]8	-0.12*	0.26**	-0.05	-0.01	0.05	-0.07	0.25**
ONI	-0.07	0.01	0.01	0.19**	0.04	0.18**	0.23**	-0.09	-0.11*	0.28**	-0.04	0.01	0.04	-0.07	0.27**
SS	0.00	0.10*	-0.02	0.04	0.02	0.06	0.02	0.05	0.00	0.01	-0.06	0.03	0.05	0.05	0.00

Table 4: Correlation between climate variables.

	SOI_St	SOI_Eq	NN12	NN3	NN4	NN34	ONI	SS
SOI_St	1.00							
SOI_Eq	0.80**	1.00						
NN12	-0.47**	-0.65**	1.00					
NN3	-0.67**	-0.83**	0.82**	1.00				
NN4	-0.69**	-0.75**	[illegible]1**	0.73**	1.00			
NN34	-0.75**	-0.85**	0.64[illegible]	0.94**	0.88**	1.00		
ONI	-0.74**	-0.85[illegible]	0.63*	0.92**	0.88**	0.99**	1.00	
SS	-0.02	-0.04	-0.02	-0.02	-0.03	-0.03	-0.03	1.00

5 Causality Analyses Comparison

The causality detection between natural inflow and climate variables in Brazil are here evaluated and compared by implying different causality detection methods summarized in section 2. It is of note that all the results were obtained using R.

5.1 Time Domain Granger Causality Test

Given the significant and empirical role of GC causality test, the GC test results are firstly conducted and summarized as follows in Table 5. It is of note that the preconditions of time domain GC test are satisfied for all tests across various combinations of variables and the corresponding optimal lag is determined respectively by a group of information criteria. Specifically, the results that are highlighted in red represent that the valid evidence is obtained for unidirectional causality from corresponding climate variable to the natural inflow. Note that these valid cases have no conflicts of causality for the reverse direction and all shows significance level less than 10%.

It is observed that the GC test shows relatively promising performance for NN12 and ONI across climate variables, for AMZ, URU and SAT among all natural inflow series. However,

there are general misleading results of the reverse direction and many cases of mutual directional causality with high significant levels.

5.2 Frequency Domain Causality Test

The frequency domain test extends the GC test and further investigates into the causal links by each particular frequency. Note that the preconditions are stratified and the optimal lag-structures are maintained for all tests. As can be seen in Table 6, the valid cases are again highlighted in red, which indicates unidirectional causality from climate variable to natural inflow without the evidence of causality for the other direction.

In general, NN34 and ONI obtain overall valid evidences of unidirectional causality without misleading results, whilst only AMZ out of all the natural inflow series shows identical valid results with NN12, NN4 and NN34. Even P2, P3, IGU, URU and SAT indicate a few valid unidirectional causality cases, however, it is not consistent and solid enough considering the amount of misleading results showing causality in reverse direction or mutual direction.

Table 5: Time domain GC test results.

	SOI_St			SOI_Eq			NN12			NN3			NN4			NN34			ONI			SS		
		lag	resault		lag	resault		lag	resault		lag	resault		lag	resault		lag	resault		lag	resault		lag	resault
GRA	→			→			→			→			→			→			→			→		
	←			←			←	11	YES*	←	11	YES*	←			←			←			←		
P1	→			→			→			→			→			→			→			→		
	←			←			←			←			←			←			←			←		
P2	→	4		→	10	YES**	→			→			→	4	YES***	→			→			→	11	YES***
	←			←			←	2	YES***	←	3	YES***	←	4	YES*	←	3	YES***	←	4	YES**	←		
P3	→			→	6		→			→			→	4	YES**	→			→			→	11	YES*
	←	10	YES*	←	10	YES	←	2	YES***	←	2	YES***	←	4	YES**	←	4	YES***	←	2	YES***	←		
SEAT	→	6	YES*	→			→			→			→			→			→			→		
	←			←			←			←			←			←			←			←		
SF	→			→			→			→			→			→			→			→		
	←			←			←			←			←			←			←			←		
P4	→			→			→			→			→			→			→			→		
	←	12	YES*	←			←	12					←			←			←			←		
AMZ	→	12	YES**	→	12	YES*	→			→			→			→			→			→		
	←	12	YES***	←	12	YES***	←	11	YES***	←	11	Yes***	←	6	YES**	←	12	YES***	←	11	YES***	←	12	YES**
TOC	→	12	YES*	→			→			→			→			→			→			→		
	←	6	YES***	←	6	YES**	←	12	YES*	←			←			←			←			←		
EAT	→			→			→			→			→			→			→			→		
	←			←			←			←			←			←			←			←		
TIE	→			→			→			→			→	1	YES**	→	12	YES**	→			→		
	←	12	YES*	←			←			←			←			←			←			←		
IGU	→			→	11	YES*	→			→	2	YES	←			→			→			→		
	←	11	YES**	←	11	YES***	←	2	YES***	←	2	YES***	←	4	YES*	←	3	YES***	←	2	YES***	←	6	YES**
URU	→			→			→			→	2	YES**	→			→			→			→		
	←	11	YES**	←	6	YES***	←	2	YES***	←	2	YES***	←	2	YES*	←	3	YES***	←	2	YES***	←	6	YES**
SAT	→			→			→			→	2	YES**	→			→			→			→		
	←	11	YES**	←	6	YES***	←	2	YES***	←	2	YES***	←	2	YES	←		YE	←	2	YES***	←		
P5	→			→	12	YES*	→			→			→			→			→			→		
	←			←	6	YES***	←			←			←			←			←			←		

←: causality from climate variable to natural inflow.
→: causality from natural inflow to climate variable.
empty cell: no causality detected.
*,**,***: indicate 10%, 5% and 1% significant level respectively.

ACCEPTED MANUSCRIPT

Table 6: Frequency domain causality test results.

	SOI_St			SOI_Eq			NN12			NN3			NN4			NN34			ONI			SS		
		freq	Y/N		freq	Y/N		freq	Y/N		freq	Y/N		freq	Y/N		freq	Y/N		freq	Y/N		freq	Y/N
GRA	→			→			→			→			→			→			→			→		
	←			←			←			←			←			←			←			←		
P1	→			→			→			→			→			→			→			→		
	←			←			←			←			←			←			←			←		
P2	→	>6		→			→			→			→	all	Y	→			→			→	2-2.5	Y
	←			←			←	>7	Y	←	>10.5	Y	←			←	>12.6	Y	←	>12.6	Y	←		
P3	→			→			→			→			→	>12.6	Y	→			→			→		
	←			←			←	>7	Y	←	>7.9	Y	←	>15.7	Y	←	>9	Y	←	>9	Y	←		
SEAT	→	2-3.1	Y	→			→			→			→			→			→			→		
	←			←			←			←			←			←			←			←		
SF	→			→			→			→			→			→			→			→		
	←			←			←			←			←			←			←			←		
P4	→			→			→			→			→			→			→			→		
	←			←			←			←			←			←			←			←		
AMZ	→			→			→			→			→			→			→			→		
	←			←			←	a	Y	←			←	3.1-6.3	Y	←	>12.6	Y	←			←		
TOC	→	3.1	Y	→			→	4.2	Y	→			→			→			→			→		
	←	3.5-5.2	Y	←			←			←			←			←			←			←		
EAT	→	2-3.5	Y	→			→	4.2-12.6	Y	→			→			→			→			→		
	←			←			←			←			←			←			←			←		
TIE	→			→			→			→			→			→			→			→	2-2.5	Y
	←			←	2-2.6	Y	←			←			←			←			←			←		
IGU	→			→			→			→	4.2-6.3	Y	→	.6	Y	→			→			→		
	←			←			←	2-3.5 or >7	Y	←	>7.9	Y	←			←	>9	Y	←	>10.5	Y	←	2-3.1	Y
URU	→			→			→			→	>6.3	Y	→			→			→			→		
	←			←			←	2-4.8 or >6.3	Y	←	>7.9	Y	←	31.4	Y	←	>7.9	Y	←	>7.9	Y	←	2-5.2	Y
SAT	→			→			→			→	>12.6	Y	→			→			→			→		
	←			←			←	2-4.2 or >7	Y	←	>7.9	Y	←	>6..8	Y	←	>7.9	Y	←	>7.9	Y	←		
P5	→			→			→	2.6-4.5	Y	→			→			→			→			→		
	←	all	Y	←	all	Y	←			←			←	>3.1	Y	←			←			←		

←: causality from climate variable to natural inflow.
→: causality from natural inflow to climate variable.
empty cell: no causality detected.
*,**,***: indicate 10%, 5% and 1% significant level respectively.

5.3 CCM

The CCM causality test has the significant advantage of no prior linear model assumptions are made and this technique is designed for better understanding of causal relationships in complex dynamical system. The results of CCM tests are briefly summarized in Table 7,Table 8 and Table 9 and organized by each pair of tested variables. Moreover, the time lag has been involved to the evaluation, where lag 1 to 6 are considered covering 6 months of lag effect. It is of note that all test results are obtained by the optimal embedding dimension respectively, which is determined by the nearest neighbor forecasting performance using simplex projection and leave-one-out cross validation is applied for the best choice on library size with optimal performance.

The results overwhelmingly indicate causality from natural inflow to climate variable[2], whilst only 18% of the pairs get positive evidence on unidirectional causality from climate variable to natural inflow. However, even among those 18% pairs, there are misleading results of no clear causality detected for specific time lag options. In general, SAT and SF along with NN3 and NN4 obtain relatively more positive results.

[2]This is possibly due to the over-sensitivity of CCM on noise, however, it is of note that the cross mapping skills of both directions are significantly high, indicating the strong link between natural inflow and climate variables.

Table 7: CCM causality test results (1).

	SOI_St			SOI_Eq			NN12			NN3			NN4			NN34			ONI			SS		
	Lag	**E**	**dir.**	**Lag**	**E**	**dir.**	**Lag**	**E**	**dir.**	**Lag**	**E**	**dir.**	**Lag**	**E**	**dir.**	**Lag**	**E**	**dir.**	**Lag**	**E**	**dir.**	**Lag**	**E**	**dir.**
GRA	1	5	→	1	6	→	1	2	→	1	2	→	1	2	←	1	2	→	1	2	→	1	2	→
	2	7	→	2	6	→	2	2	→	2	2	→	2	2	→	2	3	→	2	2	→	2	2	→
	3	5	→	3	5	→	3	3	→	3	2	→	3	2	←	3	2	→	3	3	→	3	2	→
	4	5	→	4	7	→	4	2	←	4	2	→	4	2	NO	4	2	→	4	2	→	4	2	→
	5	4	→	5	6	→	5	2	NO	5	2	NO	5	2	→	5	2	NO	5	3	→	5	2	→
	6	8	→	6	5	→	6	8	→	6	2	←	6	2	←	6	2	NO	6	2	→	6	2	→
P1	1	5	→	1	6	→	1	2	→	1	2	→	1	2	→	1	2	→	1	2	→	1	2	→
	2	7	→	2	6	→	2	2	←	2	2	→	2	2	→	2	3	→	2	2	→	2	2	→
	3	5	→	3	5	→	3	3	→	3	2	→	3	2	→	3	2	→	3	3	→	3	2	→
	4	5	→	4	7	→	4	2	←	4	2	→	4	2	→	4	2	→	4	2	→	4	2	→
	5	4	→	5	6	→	5	2	NO	5	2	←	5	2	→	5	2	→	5	3	→	5	2	→
	6	8	→	6	5	→	6	8	→	6	2	←	6	2	→	6	2	→	6	2	→	6	2	→
P2	1	5	→	1	6	→	1	2	→	1	2	→	1	2	NO	1	2	→	1	2	→	1	2	→
	2	7	→	2	6	→	2	2	→	2	2	→	2	2	→	2	3	→	2	2	→	2	2	→
	3	5	→	3	5	→	3	3	→	3	2	→	3	2	→	3	2	→	3	3	→	3	2	→
	4	5	→	4	7	→	4	2	NO	4	2	→	4	2	→	4	2	→	4	2	→	4	2	→
	5	4	→	5	6	→	5	2	NO	5	2	→	5	2	→	5	2	→	5	3	→	5	2	→
	6	3	→	6	5	NO	6	8	→	6	2	→	6	2	→	6	2	→	6	2	→	6	2	→
P3	1	5	→	1	6	→	1	2	→	1	2	→	1	2	→	1	2	→	1	2	→	1	2	→
	2	7	→	2	6	NO	2	2	→	2	2	→	2	2	→	2	3	→	2	2	→	2	2	→
	3	5	→	3	5	→	3	3	→	3	←	3	2	→	3	2	→	3	3	→	3	2	→
	4	5	→	4	7	→	4	2	→	4	2	→	4	2	→	4	2	→	4	2	→	4	2	→
	5	4	→	5	6	→	5	2	→	5	2	→	5	2	→	5	2	→	5	3	→	5	2	→
	6	8	→	6	5	→	6	8	→	6	2	→	6	2	→	6	2	→	6	2	→	6	2	→
SEAT	1	5	→	1	6	→	1	2	→	1	2	→	1	2	←	1	2	→	1	2	→	1	2	→
	2	7	→	2	6	→	2	2	→	2	2	→	2	2	→	2	3	→	2	2	→	2	2	→
	3	5	→	3	5	→	3	3	→	3	2	→	3	2	→	3	2	→	3	3	→	3	2	→
	4	5	→	4	7	→	4	2	→	4	2	→	4	2	→	4	2	→	4	2	→	4	2	→
	5	4	→	5	6	→	5	2	→	5	2	→	5	2	→	5	2	→	5	3	→	5	2	→
	6	8	→	6	5	→	6	8	→	6	2	→	6	2	→	6	2	→	6	2	→	6	2	→

←: causality from climate variable to natural inflow.
→: causality from natural inflow to climate variable.
NO: no causality detected.

ACCEPTED MANUSCRIPT

Table 8: CCM causality test results (2).

	SOI_St			SOI_Eq			NN12			NN3			NN4			NN34			ONI			SS		
	Lag	**E**	**dir.**	**Lag**	**E**	**dir.**	**Lag**	**E**	**dir.**	**Lag**	**E**	**dir.**	**Lag**	**E**	**dir.**	**Lag**	**E**	**dir.**	**Lag**	**E**	**dir.**	**Lag**	**E**	**dir.**
SF	1	5	→	1	6	→	1	2	→	1	2	→	1	2	←	1	2	→	1	2	→	1	2	→
	2	7	→			→	2	2	→	2	2	→	2	2	→	2	3	→	2	2	NO	2	2	→
	3	5	→	3	5	→	3	3	→	3	2	→	3	2	←	3	2	NO	3	3	→	3	2	→
	4	5	→	4		→	4	2	←	4	2	←	4	2	←	4	2	NO	4	2	NO	4	2	→
	5	4	→	5	6	→	5	2		5	2	←	5	2	→	5	2	NO	5	3	→	5	2	→
	6	8	→	6	5	→	6	8	→	6	2	←	6	2	→	6	2	NO	6	2	→	6	2	→
P4	1	5	→	1	6	→	1	2	→	1	2	→	1	2	→	1	2	→	1	2	→	1	2	→
	2	7	→	2	6	→	2		→	2	2	→	2	2	→	2	3	→	2	2	→	2	2	→
	3	5	→	3	5	→	3	3				→	3	2	→	3	2	→	3	3	→	3	2	→
	4	5	→	4	7	→	4	2		4	2		4	2	→	4	2	→	4	2	→	4	2	→
	5	4	→	5	6	→	5	2	→	5	2		5	2	→	5	2	→	5	3	→	5	2	→
	6	8	→	6	5	→	6	8	→	6	2	→	6	2	→	6	2	→	6	2	→	6	2	→
AMZ	1	5	→	1	6	→	1	2	→	1		→		2	→	1	2	→	1	2	→	1	2	→
	2	7	→	2	6	→	2	2	→	2	2	→	2	2	→	2	3	→	2	2	→	2	2	→
	3	5	→	3	5	→	3	3	→	3	2	→	3	2	→	3	2	→	3	3	→	3	2	→
	4	5	→	4	7	→	4	2	→	4	2	→				4	2	→	4	2	→	4	2	→
	5	4	→	5	6	→	5	2	→	5	2	→	5	2	→	5	2	→	5	3	→	5	2	→
	6	8	←	6	5	→	6	8	→	6	2	→	6	2	→	6	2	→	6	2	→	6	2	→
TOC	1	5	→	1	6	→	1	2	→	1	2	→	1	2	←		2	−	1	2	→	1	2	→
	2	7	→	2	6	→	2	2	→	2	2	→	2	2	→	2	2	→	2	2	→	2	2	→
	3	5	→	3	5	→	3	3	→	3	2	→	3	2	→	3		→		3	→	3	2	→
	4	5	→	4	7	→	4	2	→	4	2	→	4	2	→	4	2	→	4		→	4	2	→
	5	4	→	5	6	→	5	2	→	5	2	→	5	2	→	5	2	→	5	3	→	5	2	→
	6	8	→	6	5	→	6	8	→	6	2	→	6	2	→	6	2		6	2	→	6	2	→
EAT	1	5	→	1	6	→	1	2	NO	1	2	→	1	2	→	1	2	→	1		→	1	2	→
	2	7	→	2	6	→	2	2	→	2	2	→	2	2	→	2	3	→	2		→	2	2	→
	3	5	→	3	5	→	3	3	→	3	2	→	3	2	→	3	2	→	3	3	→	3	2	→
	4	5	NO	4	7	→	4	2	NO	4	2	→	4	2	→	4	2	→	4	2	→	4	2	→
	5	4	→	5	6	→	5	2	NO	5	2	→	5	2	→	5	2	→	5	3	→			→
	6	8	→	6	5	→	6	8	→	6	2	NO	6	2	→	6	2	→	6	2	→	6		

←: causality from climate variable to natural inflow.
→: causality from natural inflow to climate variable.
NO: no causality detected.

Table 9: CCM causality test results (3).

	S_St			S_Eq			NN12			NN3			NN4			NN34			ONI			SS		
	Lag	**E**	**dir.**	**Lag**	**E**	**dir.**	**Lag**	**E**	**dir.**	**Lag**	**E**	**dir.**	**Lag**	**E**	**dir.**	**Lag**	**E**	**dir.**	**Lag**	**E**	**dir.**	**Lag**	**E**	**dir.**
TIE	1	5	→	1	6	→	1	2	→	1	2	→	1	2	→	1	2	→	1	2	→	1	2	→
	2	7	→			→		2	→	2	2	→	2	2	→	2	3	→	2	2	→	2	2	→
	3	5	→	3	5	→	3	3	→	3	2	→	3	2	→	3	2	→	3	3	→	3	2	→
	4	5	→	4		→	4	2	←	4	2	→	4	2	→	4	2	→	4	2	→	4	2	→
	5	4	→	5	6	→	5	2		5	2	→	5	2	→	5	2	→	5	3	→	5	2	→
	6	8	→	6	5	→	6	8	→	6	2	→	6	2	→	6	2	→	6	2	→	6	2	→
IGU	1	5	→	1	6	→	1	2	→	1	2	→	1	2	→	1	2	→	1	2	→	1	2	→
	2	7	→	2	6	→	2	NO		2	2	←	2	2	←	2	3	→	2	2	←	2	2	→
	3	5	→	3	5	→	3	3				→	3	2	←	3	2	→	3	3	→	3	2	→
	4	5	→	4	7	→	4	2	N	4	2	NO	4	2	→	4	2	→	4	2	→	4	2	→
	5	4	→	5	6	→	5	2	→	5	2		5	2	→	5	2	→	5	3	→	5	2	→
	6	8	→	6	5	→	6	8	→	6	2	→	6	2	→	6	2	→	6	2	→	6	2	→
URU	1	5	→	1	6	→	1	2	→	1	NO		1	2	←	1	2	→	1	2	←	1	2	→
	2	7	→	2	6	→	2	2	→	2	2	→	2	2	←	2	3	→	2	2	→	2	2	→
	3	5	→	3	5	→	3	3	→	3	2	→	3	2	→	3	2	→	3	3	→	3	2	→
	4	5	→	4	7	→	4	2	→	4	2	NO			N	4	2	→	4	2	NO	4	2	→
	5	4	→	5	6	→	5	2	→	5	2	→	5	2	→	5	2	→	5	3	→	5	2	→
	6	8	→	6	5	→	6	8	→	6	2	→	6	2	→	6	2	→	6	2	→	6	2	→
SAT	1	5	→	1	6	→	1	2	→	1	2	←	1	2	←		2	←	1	2	←	1	2	→
	2	7	→	2	6	→	2	2	→	2	2	←	2	2	←	2	3	→	2	2	←	2	2	→
	3	5	→	3	5	→	3	3	→	3	2	←	3	2	→	3		→		3	→	3	2	→
	4	5	→	4	7	→	4	2	→	4	2	←	4	2	←	4	2	→	4		←	4	2	→
	5	4	→	5	6	→	5	2	→	5	2	NO	5	2	←	5	2	NO	5	3	→	5	2	→
	6	8	→	6	5	→	6	8	→	6	2	→	6	2	→	6	2		6	2	→	6	2	→
P5	1	5	→	1	6	→	1	2	→	1	2	→	1	2	→	1	2	→	1		→	1	2	NO
	2	7	→	2	6	→	2	2	→	2	2	→	2	2	→	2	3	→	2		→	2	2	→
	3	5	→	3	5	→	3	3	→	3	2	→	3	2	→	3	2	→	3	3	→	3	2	→
	4	5	→	4	7	→	4	2	→	4	2	→	4	2	→	4	2	→	4	2	→	4	2	→
	5	4	→	5	6	→	5	2	→	5	2	→	5	2	→	5	2	→	5	3	→			→
	6	8	→	6	5	→	6	8	→	6	2	→	6	2	→	6	2	→	6	2	→	6	2	

←: causality from climate variable to natural inflow.
→: causality from natural inflow to climate variable.
NO: no causality detected.

5.4 SSA based Causality Test

Follow the brief introduction of SSA based causality test in section 3, the test results of natural inflow and climate variable in Brazil are summarized in Table 10[3]. It is of note that both recurrent and vector forecasting algorithms are evaluated respectively; the out-of-sample is defined as the last 1/3 of the total observation for both SSA and MSSA forecasting; the root mean square error (RMSE) of forecasting for SSA and MSSA are the optimal outcome obtained respectively with the optimal window length (L) and numbers of eigenvalues (r) that are also listed in the table; causality is detected if the corresponding F statistics is smaller than 1 and the significant level of causality increases while the value of F statistics decreases.

In general, the results are again a mixture of different unidirectional causality, mutual directional causality and no causality, and no significant pattern can be identified, except that NN34 and NN4 work slightly better among all series. Moreover, the F statistics are very close to 1, which indicate that the forecasting of MSSA by involving the other variable is improved by a very limited amount comparing to the performance of univariate SSA.

[3]It is of note that the listed pairs are part of all combinations that cover almost all tested series and types of results. The complete details of these results are available upon request from the authors.

Table 10: SSA based causality test results.

	SSA				MSSA				SSA Causality			
	Rec		Vec		Rec		Vec		Rec	Vec		
	L,r	RMSE	L,r	RMSE	L,r	RMSE	L,r	RMSE	F stat	F st.	irection	Decision
ONI	3,2	0.21	16,14	0.20	9,6	0.20	3,2	0.21	0.92	1.09	URU caus ONI	Wrong
URU	12,3	1349.63	3,1	1357.71	2,1	1426.68	2,1	1426.68	1.06	1.0	ONI caus URU	
NN34	3,2	0.28	3,2	0.28	3,2	0.28	3,2	0.29	1.02	1.0	SAT caus NN34	No
SAT	20,5	541.68	20,10	544.38	11,3	556.97	12,3	559.69	1.03	1.03	NN34 caus SAT	
SS	16,14	1.00	16,11	1.22	8,6	1.19	8,6	1.47	1.20	1.1	P4 caus SS	Yes
P4	19,4	100.14	17,5	106.68	19,4	85.11	15,4	91.61	0.8	0.86	SS caus P4	
SOI_St	2,1	0.74	3,1	0.73	2,1	0.69	2,1	0.69	.93	0.94	SAT caus SOI_St	Wrong
SAT	20,5	541.68	20,10	544.38	11,3	556.97	12,3	559.69	1.03	1.03	SOI_St caus SAT	
NN3	3,2	0.34	3,2	0.35	3,2	0.33	3,2	0.34	0.9	.96	IGU caus NN3	Wrong
IGU	18,1	1292.42	20,1	1282.83	17,1	1338.35	19,1	1315.74	1.04	1.03	NN3 caus IGU	
NN4	6,3	0.20	17,8	0.21	3,2	0.22	3,2	0.22	1.06	1.07	GRA caus NN4	No
GRA	19,5	829.02	13,3	821.12	19,5	844.93	17,5	854.13	1.02	1.04	NN4 caus GRA	
NN12	3,2	0.57	3,2	0.57	8,5	0.49	9,6	0.5	0.86	0.83	SF caus NN12	Mutual
SF	12,5	1529.22	13,3	1509.66	20,3	1395.22	16,6	1425.42	0.91	0.94	NN12 caus SF	
NN34	3,2	0.28	3,2	0.28	3,2	0.28	3,2	0.29	1.01	1.02	P2 caus NN34	Yes
P2	20,7	1223.53	20,7	1224.24	16,7	1111.85	12,4	1088.23	0.91	0.89	NN34 caus P2	
ONI	3,2	0.21	16,14	0.20	5,4	0.19	5,4	0.2	0.88	1.03	P3 caus ONI	Mutual
P3	20,5	1330.56	5,1	1320.23	20,6	1307.70	15,4	1306.01	0.98	0.99	ONI caus P3	
NN34	3,2	0.28	3,2	0.28	3,2	0.28	3,2	0.2	1.01	1.02	AMZ caus NN34	Yes
AMZ	13,6	5052.20	20,12	4762.11	10,7	4904.91	1	4678.68	0.97	0.98	NN34 caus AMZ	
NN4	6,3	0.20	17,8	0.21	3,2	0.22	3,2	0.22	1.06	1.06	SAT caus NN4	No
SAT	20,5	541.68	20,10	544.38	11,3	556.97	12,3	5 .69	1.03	1.03	NN4 caus SAT	
NN3	3,2	0.34	3,2	0.35	3,2	0.33	3,2	0.34	0.96	0.97	P1 caus NN3	Wrong
P1	20,5	1049.30	13,3	1029.57	20,5	1047.73	1 ,5	1053.18	1.00	1.02	NN3 caus P1	
SOI_Eq	2,1	0.52	2,1	0.52	7,3	0.5	7,	0.55	1.05	1.05	URU caus SOI_Eq	No
URU	12,3	1349.63	3,1	1357.71	2,1	1426.6	17,10	1385.08	1.06	1.02	SOI_Eq caus URU	
NN4	6,3	0.20	17,8	0.21	3,2	0.22	8,	0.23	1.10	1.12	TOC caus NN4	Yes
TOC	11,5	5595.27	20,12	5229.04	15,10	4728.45	5,10	4358.17	0.81	0.83	NN4 caus TOC	
NN12	3,2	0.57	3,2	0.57	10,6	0.49	9,6	0.50	0.86	0.87	TIE caus NN12	Wrong
TIE	16,4	642.53	16,5	633.07	12,6	729.9	19,14	702.37	1.14	1.11	NN12 caus TIE	
SOI_St	2,1	0.74	3,1	0.73	8,3	0.69	8,3	0.68	0.93	0.93	IGU caus SOI_St	Wrong
IGU	18,1	1292.42	20,1	1282.83	17	1338.35	18,1	1315.74	1.04	1.03	SOI_St caus IGU	
ONI	3,2	0.21	16,14	0.20	6	0.17	8,6	0.18	0.82	0.92	SF caus ONI	Mutual
SF	12,5	1529.22	13,3	1509.66	0.3	139 22	16,6	1425.42	0.91	0.94	ONI caus SF	
NN12	3,2	0.57	3,2	0.57	14,3	0.48	14,9	0.48	0.83	0.84	P3 caus NN12	Mutual
P3	20,5	1330.56	5,1	1320.23	20,6	07.70	15,4	1306.01	0.98	0.99	NN12 caus P3	
SOI_Eq	2,1	0.52	2,1	0.52	5,2	0.56	5,2	0.55	1.07	1.06	P2 caus SOI_Eq	Yes
P2	20,7	1223.53	20,7	1224.2	6,7	1111.85	12,4	1088.23	0.91	0.89	SOI_Eq caus P2	

Yes: only causality from climate variable to natural inflows is detected.
Wrong: only causality from natural inflow to climate variable is detected.
No: no causality detected.
Mutual: mutual directional causality between climate variable and natural inflow.

5.5 Periodic Autoregressive Model based Causality Test

The PAR causality test results are summarized in Table 11[4] where both PAR and PARX RMSE are present when forecasting the last 1/3 of the total observation. Following the procedure describe in SSA causality test, if the corresponding F statistics is smaller than 1 then there is causality. When causality is detected in both directions the causality is not computed, and when the direction of causality is from the natural inflow in the climate variable then is computed as wrong. The causality is computed in the right decision only in six cases, but the F statistics is very close to one in most cases, showing that even when causality can be considered, the improvement of considering a climate variable it's on the edge. The only case where can be clearly found a causality is between SOI Equatorial and Paranapanema basin.

[4]It is of note that the listed pairs are part of all combinations that cover almost all tested series and types of results. The complete details of these results are available upon request from the authors.

Table 11: PAR based causality test results.

	RMSE			PAR Causality	
	PAR	PARX	F stat	Direction	Decision
GRA	1129.17	1076.456	0.953	NN4T caus GRA	Mutual
NN4	1.128	0.789	0.7	GRA caus NN4	
P2	2056.97	1235.528	0.601	SOI_Eq caus P2	Yes
SOI_Eq	1.69	1.754	1.038	No	
P3	1618.171	1369.67	0.846	ONI caus P3	
ONI	1.306	1.955	1.497	No	
P3	1618.171	1587.472	0.981	NN3 caus P3	Ye
NN3	1.56	2.199	1.409	No	
P3	1618.171	1434.836	0.887	NN4 caus P3	Yes
NN4	1.128	1.34	1.188	No	
P3	1618.171	1583.034	0.978	NN34 caus P3	Yes
NN34	1.574	2.143	1.362	No	
AMZ	8519.513	8581.495	1.007	No	Wrong
NN4	1.128	0.91	0.807	AMZ caus NN4	
TOC	6359.823	5489.439	0.863	ONI caus TOC	Mutual
ONI	1.306	1.006	0.77	TOC caus ONI	
EAT	806.574	472.349	0.586	SS caus EAT	Mutual
SS	64.101	24.251	0.378	EAT caus SS	
TIE	827.817	747.594	0.903	NN3 caus TIE	Yes
NN3	1.56	1.624	1.041	No	
IGU	1629.477	1348.128	0.827	ONI caus IGU	Mutual
ONI	1.306	0.847	0.649	IGU caus ONI	
URU	1827.213	1497.444	0.82	SOI_St caus URU	Mutual
SOI_St	1.537	1.152	0.7	URU caus SOI_St	
SAT	712.875	550.122	0.772	NN12 caus SAT	Mutual
NN12	1.606	1.406	0.876	SAT caus NN12T	
P5	193.369	196.162	1.01	No	Wrong
SOI_Eq	1.69	1.544	0.914	P5 caus SOI_Eq	

Yes: only causality from climate variable to natural inflow is detected.
Wrong: only causality from natural inflow to climate variable is detected.
No: no causality detected.
Mutual: mutual directional causality between climate variable and natural inflow.

6 Final Discussion and Conclusion

In general, this paper successfully obtains comprehensive investigation of the causality relationship between natural inflow and climate variables in Brazil by analyzing the data of 15 major basins and 8 different climate series. For the first time to the best of our knowledge, it incorporates and compares five different causality detection methods for the causality study on hydrological series. In specific, GC test shows relatively promising performance for AMZ, URU and SAT among all natural inflow series, NN12 and ONI across climate variables; frequency domain causality test indicates generally valid evidences of unidirectional causality for AMZ, NN34 and ONI; CCM overwhelmingly obtains significant unidirectional causality from the opposite direction (natural inflow to climate variables), whilst SAT, SF, NN3 and NN4 relatively give more positive results of the valid direction; SSA based causality test shows that NN34 and NN4 work slightly better, and the forecasting improvements by involving the other variable are generally very limited; PAR based causality test computed six unidirectional causality, but only one is really significant (P2 and SOI_Eq).

The overall results indicate that there is no single method which stands out and outperforms the others. The conclusions are a mixture of different unidirectional, mutual directional, and no causality. There is no obvious pattern that can be clearly identified across 15 natural inflow series and 8 climate variables. However, it is noticed that the overwhelming evidences of opposite

direction of causality are obtained by CCM, which is the most concurrent outcome of all five different tests. It is frankly interesting discovery that is possibly caused by significant noises that generally exist in those series, which will be one of the main focuses for future research.

The works presented in the Background section showed improvements when using information from the climate variables in the inflow prediction procedure, so even if the tests applied here did not present favourable results, a natural continuation of this study will be the application of different models that incorporate exogenous variables to verify the significance of the climate variables in the prediction of each of the inflow series studied.

References

[1] Operador Nacional do Sistema Elétrico (2017). www.ons.co n.br.

[2] Amarasekera, K., Lee, R., Willians, E. & Eltahir, E. (1997) ENSO and natural variability in the flow of tropical rivers. Journal of Hydrology, 200, 24–39.

[3] Dettinger, M. & Diaz, H. (2000). Global characteristics of streamflow seasonality and variability. Journal of Hydrometeorology, 1, 289–310.

[4] Foley, J., Botta, A., Coe, M. & Costa, M. (2002). El Niño-Southern oscillation and the climate, ecosystems and rivers of Amazonia. Global Biogeochemical Cycles, 16, 1132.

[5] Berri, G., Ghietto, M. & García, N. (2000). The Influence of ENSO in the flows of the Upper Paraná River of South America over the Past 100 Years. Journal of Hydrometeorology, 3, 57–65.

[6] Garcia, N. & Mechoso, C. (2005). Variability in the discharge of South American rivers and in climate. Hydrological Sciences Journal, 3, 459–478.

[7] Stuck, J., Güntner, A. & Merz, B. (2006). ENSO impact on simulated South American hydro-climatology. Advances in Geosciences, 6, 227–236.

[8] Soares, J., Carriello, F., Ferreira, N. & Rennó, C. (2006). Mapping the hydrologic response of the Brazilian hydrologic regions and their variability associated with El Niño and La Niña. Revista Ambiente & Água, 1, 21–36.

[9] Ausloos, M., & Ivanova, K. (2001). Power-law correlations in the southern-oscillation-index fluctuations characterizing El Niño. Physical Review E, 63(4), 047201.

[10] Cardoso, A. & Silva Dias, P. (2006). The relationship between ENSO and Paraná River flow. Advances in Geosciences, 6, 189–193.

[11] Lima, L., Popova, E. & Damien, P. (2014). Modeling and forecasting of Brazilian reservoir inflows via dynamic linear models. International Journal of Forecasting, 30, 464–476.

[12] Maçaira, P., Cyrino Oliveira, F., Ferreira, P., de Almeida, F. & Souza, R. (2017). Introducing a Causal PAR(p) Model to Evaluate the Influence of Climate Variables in Reservoir Inflows: a Brazilian Case. Pesquisa Operacional, 37, 107–128.

[13] Silveira, C., Alexandre, A., Souza Filho, F., Vasconcelos Junior, F. & Cabral, S. (2017). Monthly streamflow forecast for National Interconnected System (NIS) using Periodic Autoregressive Endogenous Models (PAR) and Exogenous (PARX) with climate information. Brazilian Journal of Water Resources, 22, 1–10.

[14] Domino, K., Bachowicz, T., & Ciupak, M. (2014). The use of copula functions for predictive analysis of correlations between extreme storm tides. Physica A: Statistical Mechanics and its Applications, 413, 489-497.

[15] Zhang, Q., Xu, C. Y., Yu, Z., Liu, C. L., & Chen, Y. D. (2009). Multifractal analysis of streamflow records of the East River basin (Pearl River), China. Physica A: Statistical Mechanics and its Applications, 388(6), 927-934.

[16] Hurst, H. E. (1951). Long term storage capacity of reservoirs. ASCE Transactions, 116(776), 770-808.

[17] Rotundo, G., Ausloos, M., Herteliu, C., & Ileanu, B. (2015). Hurst exponent of very long birth time series in XX century Romania. Social and religious aspects. Physica A: Statistical Mechanics and its Applications, 429, 109-117.

[18] Ausloos, M., Cerqueti, R., & Lupi, C. (2017). Long-range properties and data validity for hydrogeological time series: the case of the Paglia river. Physica A: Statistical Mechanics and its Applications, 470, 39-50.

[19] Granger, C. W. (1969). Investigating causal relations by econometric models and cross-spectral methods. Econometrica: Journal of the Econometric Society, 37(3), 424-438.

[20] Breitung, J. & Candelon, B. (2006). Testing for short- and long-run causality: A frequency-domain approach. Journal of Econometrics, 132, 363-378.

[21] Sugihara, G., May, R., Ye, H., Hsieh, C. H., Deyle, E., Fogarty, M. & Munch, S. (2012). Detecting causality in complex ecosystems. Science, 338(6106), 496-500.

[22] Hassani, H., Heravi, S., & Zhigljavsky, A. (2013). Forecasting UK industrial production with multivariate singular spectrum analysis. Journal of Forecasting, 32(5), 395-408.

[23] Sanei, S. & Hassani, H. (2015). Singular spectrum analysis of biomedical signals. CRC Press.

[24] Hassani, H., & Mahmoudvand, R. (2018). Singular Spectrum Analysis: Using R. Springer.

[25] Hassani, H., Huang, X., Gupta, R. & Ghodsi, M. (2016). Does sunspot numbers cause global temperatures? A reconsideration using non-parametric causality tests. Physica A: Statistical Mechanics and its Applications, 460, 54–65. Elsevier.

[26] Terry, L., Pereira, M., Neto, T., Silva, L. & Sales, P. (1986). Coordinating the Energy Generation of the Brazilian National Hydrothermal Electrical Generating System. Interfaces, 16, 16–38.

[27] Ursu, E. & Pereau, J. (2017). Estimation and identification of periodic autoregressive models with one exogenous variable. Journal of the Korean Statistical Society, 46, 629–640.

[28] Collette, C., & Ausloos, M. (2004). Scaling analysis and evolution equation of the North Atlantic oscillation index fluctuations. International journal of modern physics C, 15(10), 1353-1366.

[29] Geweke, J. (1982). Measurement of linear dependence and feedback between multiple time series. Journal of the American Statistical Association, 77, 304-324.

[30] Huang, X., Hassani, H., Ghodsi, M., Mukherjee, Z. & Gupta, R. (2017). Do trend extraction approaches affect causality detection in climate change studies? Physica A: Statistical Mechanics and its Applications, 469, 614-624.

[31] Deyle, E., Fogarty, M., Hsieh, C., Kaufman, L., MacCall, A., Munch, S., Perretti, C., Ye, H. & Sugihara, G. (2013). Predicting climate effects on Pacific sardine. Proceedings of the National Academy of Sciences, 110(16), 6430-6435.

[32] Ye, H., Deyle, E., Gilarranz, L. & Sugihara, G. (2015). Distinguishing time-delayed causal interactions using convergent cross mapping. Scientific Reports, 5, 14750.

[33] Takens, F. (1981). Detecting strange attractors in turbulence Dynamical Systems and Turbulence. Dynamic Systems and Turbulence, 898, 366-381.

[34] Sugihara, G. & May, L. (1990). Nonlinear forecasting as a way of distinguishing chaos from measurement error in time series. Nature, 344(6268), 734-741.

[35] Hassani, H., Zhigljavsky, A., Patterson, K. & Soofi, A. (2010). A comprehensive causality test based on the singular spectrum analysis. Causality in Science, 379-406. Oxford University Press.

[36] Maceira, M. & Damázio, J. (2006). Use of the PAR(p) Model in the Stochastic Dual Dynamic Programming Optimization Scheme Used in the Operation Planning of the Brazilian Hydropower System. Probability in the Engineering and Informational Sciences, 20, 143-156.

[37] Operador Nacional do Sistema Elétrico (2016). Atualização de Séries Históricas de Vazões, período 1931 a 2015.

[38] Petroni, F., & Ausloos, M. (2008). High frequency intrinsic modes in El Nino/Southern Oscillation Index. Physica A: Statistical Mechanics and its Applications, 387(21), 5246-5254.

[39] Cimino, G., Del Duce, G., Kadonaga, L. K., Rotundo, G., Sisani, A., Stabile, G., ... & Whiticar, M. (1999). Time series analysis of geological data. Chemical geology, 161(1-3), 253-270.

- Causality between hydrological natural inflows and climate variables in Brazil.
- Data from 15 major basins in Brazil and 8 climate variables.
- Comprehensive comparison of 5 different causality detection methods.
- Evaluate both well established and novel empirical causality detection approaches.